Synthesis and Electrochemical Characterization of Binuclear Rhodium and Ruthenium Complexes with 1,8-Naphthyridine-2,7-dicarboxylate. X-ray Molecular Structure of Tris(μ-acetato)(1,8-naphthyridine-2,7-dicarboxylato)diruthenium

Jean-Paul Collin,[†] Abdelaziz Jouaiti,[†] Jean-Pierre Sauvage,[*,†] William C. Kaska,[*,‡]
Margaret A. McLoughlin,[‡] Nancy L. Keder,[‡] William T. A. Harrison,[‡] and Galen D. Stucky[‡]

The cresent-shaped ligand 1,8-naphthyridine-2,7-dicarboxylate (dcnp^{2-}) has been synthesized and treated with [Rh$_2$(OAc)$_4$] and [Ru$_2$(OAc)$_4$]Cl to give [Rh$_2$(OAc)$_3$(dcnp)]$^-$ and [Ru$_2$(OAc)$_3$(dcnp)], respectively. The mixed-valence state Ru^{III}-Ru^{II} is highly stabilized by dcnp^{2-} with a K_c value of 2.5 × 10^{24}. The X-ray molecular structure of Ru$_2$(O$_2$C$_2$H$_3$)$_3$(C$_{10}$H$_9$O$_4$N$_2$) was determined in the orthorhombic space group $Pnam$ with $a = 16.013$ (2) Å, $b = 20.792$ (3) Å, $c = 23.264$ (3) Å, and $Z = 12$ and shows a pair of ruthenium atoms 2.265 (5) Å apart that are surrounded by three acetate bridges. The trans effect of the Ru-Ru bond causes a lengthening of the Ru-O dcnp bond in the complex.

Introduction

The binucleating ligand 1,8-naphthyridine (np) has already been shown to act as a bridging ligand in several examples that involve copper,[1,2] nickel,[3] or rhodium.[4] The corresponding dinuclear complexes display specific properties, and in general, close proximity between two nuclear metal centers is expected to lead to synergic effects,[5,6] particularly in homogeneous catalysis.[7,8]

It has recently been demonstrated that homogeneous oxidation of water to dioxygen is efficiently catalyzed by a dinuclear ruthenium complex in which both ruthenium centers are bridged by an oxo ligand.[9-11] In this respect, the use of an assembling ligand to maintain the dinuclear structure of the complex throughout its catalytic reactions, seems to be promising.

Derivatives of 1,8-naphthyridine that have functional groups (2-pyridyl) at the 2- and 7-positions have also been shown to form dinuclear complexes of rhodium[12-15] and ruthenium.[16] Until now, the binucleating ligand 1,8-naphthyridine-2,7-dicarboxylate (dcnp^{2-}) has only been used once, in a nickel complex,[17] which gives [Ni$_2$(dcnp)$_3$]$^{2-}$.

In the present report, we describe the complexes obtained by treating dcnp with [Rh$_2$(OAc)$_4$] or [Ru$_2$(OAc)$_4$]$^+$. The electrochemical properties of the binuclear species are compared to those of the analogous complexes obtained with the neutral ligands dpnp and dpanp. The X-ray molecular structure of [Ru$_2$(OAc)$_3$(dcnp)] is also reported. The ligand used in the present work, dcnp^{2-}, is depicted in Chart I with the other ligands studied previously for comparison: np, dpnp,[12-14,17] and dpanp.[15]

Results and Discussion

1. Preparation of the Ligand and its Complexes. 2,7-Dimethyl-1,8-naphthyridine[18] was oxidized successively to 1,8-naphthyridine-2,7-dicarboxaldehyde and 1,8-naphthyridine-2,7-dicarboxylic acid, following the procedure described by Deady.[19] The complexes [Rh$_2$(OAc)$_3$(dcnp)]$^-$ and [Ru$_2$(OAc)$_3$(dcnp)] have been obtained by treating stoichiometric amounts of dcnp^{2-} with [Rh$_2$(OAc)$_4$][20] and [Ru$_2$(OAc)$_4$]$^+$Cl$^-$,[20] respectively. An acetato group is readily substituted at room temperature for the ruthenium complex whereas reflux in methanol is required in the case of rhodium. For both complexes obtained, the valence state is unchanged with respect to the starting complex (formally, rhodium(+2) and ruthenium(+2.5)). Elemental analyses and ^{1}H NMR spectroscopy (for [Rh$_2$(OAc)$_3$(dcnp)]$^-$) confirmed the formula. The ^{1}H NMR spectrum of the dirhodium compound shows two singlets (CH$_3$) at 2.02 and 1.49 ppm in the relative ratio of 1:2, which indicates that one acetate group is trans and the two others are cis with respect to the 1,8-naphthyridine plane of dcnp^{2-}. The structure of [Rh$_2$(OAc)$_3$(dcnp)]$^-$ is thus likely to be analogous
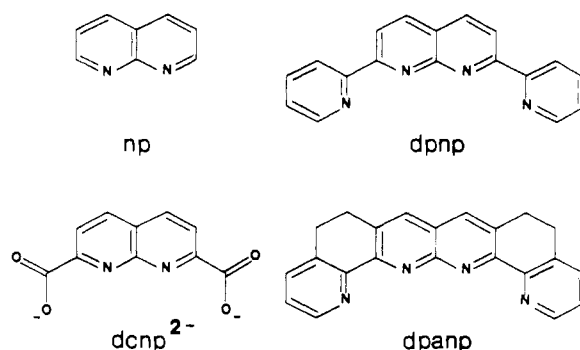
† Institut de Chimie.
‡ University of California.

Chart I

np　　　　dpnp

dcnp^{2-}　　　　dpanp

Table I. Electronic Properties of the Dirhodium and Diruthenium Complexes^a

complex	λ_{max}, nm (log ϵ)	ref
[Rh$_2$(OAc)$_4$(CH$_3$CN)$_2$]	552 (2.37), 437 (2.10)	27
[Rh$_2$(OAc)$_3$(dpnp)]$^+$	578 (3.52), 540 sh (3.40), 440 sh (3.08), 408 sh (3.34), 364 (4.63), 346 (4.46), 283 (4.33), 248 (4.69)	13
[Rh$_2$(OAc)$_3$(dpanp)]$^+$	562 (4.22), 536 (4.15), 420 (4.61), 382 (5.24), 364 (5.01), 288 (3.87), 246 (5.27), 212 (5.31)	15
^{b}[Rh$_2$(OAc)$_3$(dcnp)]$^-$	545 (3.39), 510 (3.40), 393 (2.87), 308 (4.02), 296 sh (3.97), 252 (3.98), 224 (4.27)	c
[Ru$_2$(OAc)$_4$]$^+$	1000 (1.77), 526 sh (1.08), 424 (2.87), 309 sh (3.30)	28
[Ru$_2$(OAc)$_3$(dpnp)]$^+$	917 (3.24), 729 (3.76), 612 (3.72), 351 (4.52), 287 (4.26), 274 (4.38), 246 (4.54)	16
^{b}[Ru$_2$(OAc)$_3$(dcnp)]	710 (3.22), 530 (3.18), 309 (3.92), 278 sh (3.87)	c

^{a} In CH$_3$CN at room temperature. ^{b} In methanol solution. ^{c} This work.

to that of [Rh$_2$(OAc)$_3$(dpnp)], whose structure has been determined previously,[12] and thus also similar to that of the presently

(1) Gatteschi, D.; Mealli, C.; Sacconi, L. Inorg. Chem. 1976, 15, 2774.
(2) Gatteschi, D.; Mealli, C. J. Chem. Soc., Chem. Commun. 1982, 97.
(3) Sacconi, L.; Gatteschi, D.; Mealli, C. Inorg. Chem. 1982, 21, 1985.
(4) Balch, A. L.; Cooper, R. D. J. Organomet. Chem. 1979, 169, 97.
(5) Mann, K. R.; Bell, R. A.; Gray, H. B. Inorg. Chem. 1979, 18, 2671.
(6) Kubiak, C. P.; Woodcock, C.; Eisenberg, R. Inorg. Chem. 1982, 21, 2119.
(7) Felthouse, T. R. Prog. Inorg. Chem. 1982, 29, 73.
(8) Petiniot, N.; Noels, A. F.; Anciaux, A. J.; Hubert, A. J.; Teyssie, P. Fundamental Research in Homogeneous Catalysis; Tsutsui, M., Ed.; Plenum: New York, 1979; Vol. 3, p 421.

Table II. Redox Potentials for Naphthyridine Complexes of Dirhodium and Diruthenium Acetate[a]

complex	$E_{1/2}$, V (vs SCE)				
	III,III/III,II	III,II/II,II	II,II/II,I	II,I/I,I	ref
$[Rh_2(OAc)_4(CH_3CN)_2]$		1.0	-1.08^b		29
$[Rh_2(OAc)_3(dpnp)]^+$		1.28	-0.57	-1.21	13
$[Rh_2(OAc)_3(dpanp)]^+$		1.33	-0.68	-1.36	15
$^b[Rh_2(OAc)_3(dcnp)]^-$		0.98	-0.95	-1.80	c
$[Ru_2(OAc)_4]^+$		0.05			33
$[Ru_2(OAc)_3(dpnp)]^•$		0.72	-0.62	-1.37	16
$[Ru_2(dpnp)(bpy)_2Cl_2]^{2+}$	1.34	0.64	-0.76	-1.35	16
$^b[Ru_2(OAc)_3(dcnp)]$	0.33	-1.11	-1.86^d		c

[a] At 25 °C; 0.1 M TBAP as supporting electrolyte in CH_3CN. [b] In DMF. [c] This work. [d] Irreversible reduction.
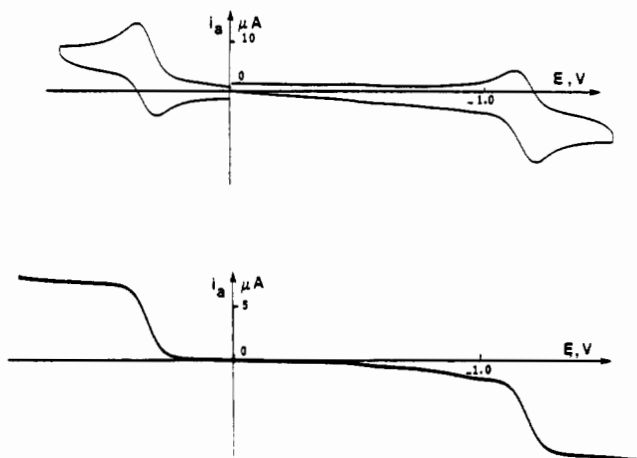

Figure 1. (a) Top: Cyclic Voltammogram of $[Ru_2(OAc)_3(dcnp)]$ in DMF (0.1 M TBAP) at a scan rate of 100 mV s⁻¹. (b) Bottom: Linear-sweep voltammogram of the same solution at a glassy-carbon rotating disk electrode. Scan rate = 4 mV s⁻¹; rotation rate = 200 rpm.

reported diruthenium complex $[Ru_2(OAc)_3(dcnp)]$.

2. Electronic Spectra. The ultraviolet and visible spectral data of the complexes prepared are given in Table I. For comparison, the spectral characteristics of related dinuclear rhodium and ruthenium complexes are also presented.

The complex $[Rh_2(OAc)_3(dcnp)]^-$ shows intense and low-energy absorption bands, which have been attributed to metal-to-ligand charge transfer (MLCT). Several studies have been devoted to the assignment of such bands.[21,22] It is likely that MLCT bands, commonly found in polypyridine complexes are also present.[23-25]

(9) Gersten, S. W.; Samuels, G. J.; Meyer, T. J. *J. Am. Chem. Soc.* **1982**, *104*, 4029.
(10) Gilbert, J. A.; Eggleston, D. S.; Wyatt, R. M., Jr.; Geselowitz, D. A.; Gersten, S. W.; Hodgson, D. J.; Meyer, T. J. *J. Am. Chem. Soc.* **1985**, *107*, 3855.
(11) Nazeeruddin, M. K.; Rotzinger, F. P.; Gratzel, M. *J. Chem. Soc., Chem. Commun.* **1988**, 872.
(12) Tikkanen, W. R.; Binamira-Soriaga, E.; Kaska, W. C.; Ford, P. C. *Inorg. Chem.* **1983**, *22*, 1147.
(13) Tikkanen, W. R.; Binamira-Soriaga, E.; Kaska, W. C.; Ford, P. C. *Inorg. Chem.* **1984**, *23*, 141.
(14) Baker, A. T.; Tikkanen, W. R.; Kaska, W. C.; Ford, P. C. *Inorg. Chem.* **1984**, *23*, 3254.
(15) Thummel, R. P.; Lefoulon, F.; Williamson, D.; Chavan, M. *Inorg. Chem.* **1986**, *25*, 1675.
(16) Binamira-Soriaga, E. Thesis, University of California, Santa Barbara, 1985.
(17) Aghabozorg, H.; Palenik, R. C.; Palenik, G. J. *Inorg. Chem.* **1985**, *24*, 4214.
(18) Paudler, C. J.; Kress, J. J. *J. Heterocycl. Chem.* **1967**, *4*, 284.
(19) Chandler, C. J.; Deady, L. W.; Reiss, J. A.; Tzimos, V. *J. Heterocycl. Chem.* **1982**, *19*, 1017.
(20) Legzdins, P.; Mitchell, R. W.; Rempel, G. L.; Ruddick, J. D.; Wilkinson, G. *J. Chem. Soc. A* **1970**, 3322.
(21) Norman, J.; Kolari, H. K. *J. Am. Chem. Soc.* **1978**, *100*, 791.
(22) Martin, D. S.; Webb, T. R.; Robbins, G. A.; Fanwich, P. E. *Inorg. Chem.* **1979**, *18*, 475.
(23) Paris, J. P.; Brandt, W. W. *J. Am. Chem. Soc.* **1959**, *81*, 5001.

The same is true for the ruthenium complex $[Ru_2(OAc)(dcnp)]$. The broad band observed at 716 nm has no equivalent in $[Ru_2(OAc)_4]^+$ and may correspond to a MLCT transition.[26]

3. Electrochemical Properties. The redox behavior of the complexes has been studied by cyclic voltammetry and by linear-sweep voltammetry with a rotating disk electrode for various rhodium and ruthenium complexes. Each electrochemical process corresponds to a one-electron transfer. The reactions are reversible with a ΔE_p value close to 60 mv (ΔE_p is the oxidation to reduction peak difference). The electrochemical data are collected in Table II. As an example, the electrochemistry of $[Ru_2(OAc)_3(dcnp)]$ is shown in Figure 1.

(a) Rhodium Complexes. For the dpnp and dpanp complexes, the $Rh^{III}Rh^{II}/Rh^{II}_2$ couple has a potential that is shifted towards positive values by $\sim$300 mV with respect to that of $[Rh_2(OAc)_4(CH_3CN)_2]^+$. This effect has been assigned to the replacement of a negatively charged acetate group by a neutral and poorly electron-donating naphthyridine ligand. By addition of two axial carboxylate groups to the complex $[Rh_2(OAc)_3(dcnp)]^-$, the III/II oxidation state is stabilized as compared to $[Rh_2(OAc)_3(dpnp)]^+$, the potential being +0.98 and +1.28 V, respectively. In analogy with other related dinuclear rhodium complexes of the type $[Rh_2(OAc)_n(L)_p]$[29] the orbitals involved in the oxidation process are associated with the Rh–Rh species.

As expected, the reduction process ($Rh^{II}_2/Rh^{II}Rh^I$) of the positively charged complexes dpnp and dpanp is facilitated as compared to the others. Like that for other rhodium complexes which have aromatic imine ligands, the reduction reaction is probably ligand localized.[29] Noteworthy is the very negative value of the $Rh^{II}Rh^I/Rh^I_2$ redox potential for $[Rh_2(OAc)_3(dcnp)]^-$ and its reversibility.

(b) Ruthenium Complexes. The most striking feature of Table II is the extremely accessible potential of the $Ru^{III}_2/Ru^{III}Ru^{II}$ couple of $[Ru_2(OAc)_3(dcnp)]$ (+0.33 V). In agreement with the remarkable stability of the high-oxidation-state systems (III,III and III,II) is the very negative value of the $Ru^{III}Ru^{II}/Ru^{II}_2$ redox potential in the same complex (−1.11 V).

When an acetate ligand is replaced with dpnp, the (III,II) state is strongly destabilized since the redox potential values for $Ru^{III}Ru^{II}/Ru^{II}_2$ are 0.06 and 0.72 V for $[Ru_2(OAc)_4]^{+/0}$ and $[Ru_2(OAc)_3(bpnp)]^{2+/+}$, respectively. The same trend is observed for $[Ru_2(bpnp)(bpy)_2Cl_2]^{3+}$. On the contrary, if an acetate is substituted for dcnp²⁻, the same $Ru^{III}Ru^{II}/Ru^{II}_2$ couple is strongly shifted to negative potentials.

The mixed-valence state Ru^{III}–Ru^{II} is highly stabilized by dcnp²⁻. According to the classification of Robin and Day,[30] $[Ru_2(OAc)_3(dcnp)]$ belongs to class III compounds, due to strong

(24) Lytle, F. E.; Hercules, D. M. *J. Am. Chem. Soc.* **1969**, *91*, 263.
(25) Van Houten, J.; Watts, R. J. *J. Am. Chem. Soc.* **1976**, *98*, 4853.
(26) Staniewicz, R. J.; Sympson, R. F.; Hendricker, D. G. *Inorg. Chem.* **1977**, *16*, 2166.
(27) Johnson, S. A.; Hunt, H. R.; Newman, H. M. *Inorg. Chem.* **1963**, *2*, 960.
(28) Stephenson, T. A.; Wilkinson, G. *J. Inorg. Nucl. Chem.* **1966**, *28*, 2285.
(29) Le, J. C.; Chavan, M. Y.; Chau, L. K.; Bear, J. L.; Kadish, K. M. *J. Am. Chem. Soc.* **1985**, *107*, 7195.
(30) Chakravarty, A. K.; Cotton, F. A. *Inorg. Chem.* **1986**, *25*, 21430. Robin, M. B.; Day, P. *Adv. Inorg. Chem. Radiochem.* **1967**, *10*, 247.

Table III. Cell Constants and Crystallographic Data

mol formula	$Ru_2C_{16}H_{13}O_{10}N_2 \cdot 2H_2O$
fw	631.41
space group	*Pnam*
Z	12
a,^{a} Å	16.013 (2)
b,^{a} Å	20.792 (3)
c,^{a} Å	23.264 (3)
α, deg	90
β, deg	90
γ, deg	90
V, Å^3	7745
d (calcd), g/cm^3	1.62
radiation type; wavelength, Å	Mo; 0.7107
temp, °K	298
abs coeff, cm^{-1}	12.0
R, %	7.99
R_w, %	9.76

^{a} With esd's in parentheses.

Table IV. Selected Bond Distances and Angles for [Ru$_2$(OAc)$_3$(dcnp)]

Distances (Å)			
Ru(1)–Ru(1)	2.273 (4)	C(141)–C(142)	1.48 (3)
Ru(1)–N(142)	2.00 (3)	C(141)–O(141)	1.24 (1)
Ru(1)–O(142)	2.28 (1)	C(132)–O(132)	1.26 (3)
Ru(1)–O(132)	2.06 (1)	C(140)–C(145)	1.42 (4)
Ru(1)–O(112)	2.05 (1)	C(140)–N(142)	1.37 (3)
Ru(1)–O(122)	2.03 (1)	C(132)–C(133)	1.57 (4)

Angles (deg)			
O(112)–Ru(1)–Ru(1)	89.6 (4)	O(142)–Ru(1)–O(122)	87.0 (6)
O(122)–Ru(1)–Ru(1)	90.0 (4)	O(142)–Ru(1)–O(132)	103.8 (6)
O(132)–Ru(1)–Ru(1)	89.4 (4)	N(142)–Ru(1)–Ru(1)	90.3 (5)
O(132)–Ru(1)–O(112)	87.0 (6)	N(142)–Ru(1)–O(112)	89.6 (6)
O(132)–Ru(1)–O(122)	90.5 (6)	N(142)–Ru(1)–O(122)	93.0 (6)
O(142)–Ru(1)–Ru(1)	166.5 (4)	N(142)–Ru(1)–O(132)	176.6 (6)
O(142)–Ru(1)–O(112)	93.9 (6)	N(142)–Ru(1)–O(142)	76.7 (7)

interaction between the metal centers. The stability of the intervalent (III,II) state can be estimated by its redox existence range (−1.11 to +0.33 V). A better measure is the value of the comproportionation constant K_c of equilibrium (1). The constant

$$Ru^{II}-Ru^{II} + Ru^{III}-Ru^{III} \overset{K_c}{\rightleftharpoons} 2Ru^{II}-Ru^{III} \qquad (1)$$
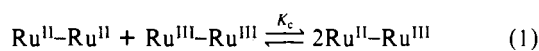
K_c can be estimated by

$$\log K_c = \frac{\mathscr{F}}{RT}(E_2° - E_1°)$$

where $E_2°$ and $E_1°$ are the redox potentials of the $Ru^{III}_2/Ru^{III}Ru^{II}$ and $Ru^{III}Ru^{II}/Ru^{II}_2$ couples respectively (+0.33 and −1.11 V). The complex [Ru$_2$(OAc)$_3$(dcnp)] has a K_c value of 2.5 × 10^{24}. It is thus one of the most stable $Ru^{III}-Ru^{II}$ mixed-valence complexes that belong to class III. Another example of a highly stable $Ru^{III}-Ru^{II}$ complex is that of [Ru$_2$(napy)$_2$(dpnp)(μ-Cl)$_2$]$^{3+}$,[16] which has a comproportionation constant K_c of 3.5 × 10^{23}. These two complexes stress the importance of bridging aromatic ligands in electronic delocalization over the two metal centers.

By comparison with other analogous rhodium and ruthenium complexes, the irreversible reduction wave corresponding to [Ru$_2$(OAc)$_3$(dcnp)]$^{-1/2-}$ (formally $Ru^{II}_2/Ru^{II}Ru^{I}$) is highly negative (−1.86 V) and may be assigned to the addition of an electron to ligand- (dcnp^{2-}-) centered orbitals.

4. X-ray Molecular Structure of the Complex [Ru$_2$(OAc)$_3$-(dcnp)]. The final atomic positional and thermal parameters for the complex are shown in Table V (supplementary material). There are three distinct ruthenium sites with one and one-half unique molecules in the unit cell, where the half-molecule lies on a mirror plane. An ORTEP drawing of the molecule is shown in Figure 2 with the atom numbering scheme of the molecule on the mirror plane. Selected bond lengths and angles are presented in Table IV.

The X-ray molecular structure shows a pair of ruthenium atoms bridged by dcnp and three acetate ligands with an octahedral geometry about each metal center. The average of the Ru(1)–Ru(1) and, Ru(2)–Ru(3) bond distances is 2.265 (5) Å, which
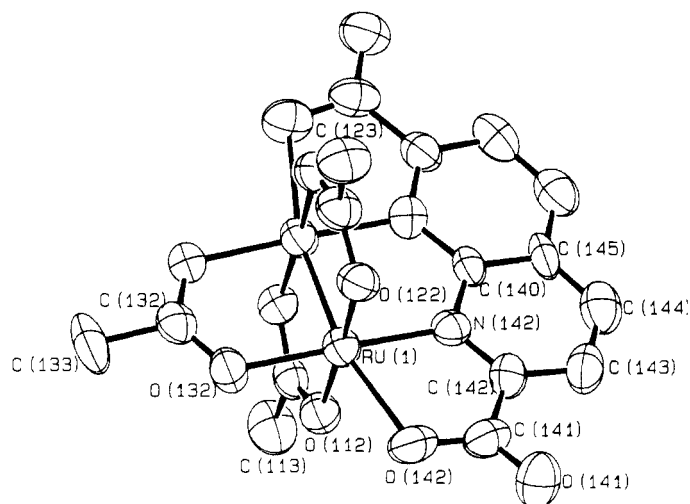
Figure 2. ORTEP diagram of [Ru$_2$(OAc)$_3$(dcnp)]. The numbering scheme corresponds to atomic positions in Table IV; 50% probability ellipsoids are shown.

is within the range of distances (2.238–2.408 Å) observed for metal–metal-bonded diruthenium complexes derived from the parent tetracarboxylates,[31] it is one of the shortest metal–metal-bonded diruthenium complexes based on naphthyridine,[16] but the distance compares well with the 2.267 Å length for [Ru$_2$(O-Ac)$_4$]Cl·2H$_2$O, which is a II/III complex.[31] Evidently the substitution by a carboxylate group on dcnp for acetates on the ruthenium complex does not change the metal–metal distance significantly. This is similar to the tris(μ-acetato)(2,7-bis(2-pyridyl)-1,8-naphthyridine)dirhodium(III) hexafluorophosphate where the naphthyridine replaces a bridging acetate on dirhodium tetracetate. Here the Rh–Rh distance lengthens by only 0.01 Å over that of the tetracetate complex. In addition the Ru–N-(naphthyridine) distance is on the average 2.02 (4) Å, which is shorter than the average for [Ru$_2$(OAc)$_3$(dpnp)]$^+$, 2.04 Å.

The ruthenium acetate distances (Ru–O) are similar to those in [Ru$_2$(OAc)$_4$]Cl, with the Ru–O(142) bond trans to the Ru–Ru bond being much longer than the other Ru–O bonds probably because of the trans influence of the Ru–Ru bond. A similar effect occurs with the [Ru$_2$(OAc)$_3$(dpnp)]$^+$PF$_6^-$ complex.[16] Here the Ru–N(pyridine) is 2.238 Å. Most Ru–N(pyridine) distances are in the range 2.040–2.067 Å.[32]

Experimental Section

Materials. The chemicals used were of reagent grade quality and were used without purification. Acetonitrile (Merck, spectroscopic quality) was used as received. DMF (Prolab) was dried overnight over alumina, distilled under reduced pressure, and stored under argon. RuCl$_3$·3H$_2$O and RhCl$_3$·3H$_2$O were obtained from Aldrich.

Physical Measurements. The ^{1}H NMR spectra were performed on a Bruker WP 200 SY spectrometer; the chemical shifts were measured versus tetramethylsilane as a reference. Ultraviolet–visible spectra were taken on a Kontron (Uvicon) apparatus. Cyclic and linear-sweep voltammetry measurements were carried out on the Bruker EI 310 M potentiostat connected to a XY IFELEC 3802 recorder. The experiments were done under argon, after 20 min of degassing, in a three-electrode cell. The working electrodes used were glassy carbon or platinum (Tacussel). The temperature was 22 °C, and the potentials were measured versus the saturated sodium chloride calomel electrode (SSCE). The reference electrode was separated from the solution by a length of tubing that contained a low-porosity frit and 0.1 M tetra n-butylammonium perchlorate (TBAP) solution in CH$_3$CN. The supporting electrolyte was TBAP (Fluka); it was dried overnight at 70 °C.

Preparation of Ligands and Complexes. 2,7-Dimethyl-1,8-naphthyridine and 1,8-naphthyridine-2,7-dicarboxylic acid (dcnpH$_2$) were prepared according to literature procedures.[17,18] [Ru$_2$(OAc)$_4$]Cl and

(31) Cotton, F. A.; Walton, R. A. *Multiple Bonds Between Metal Atoms*; John Wiley and Sons: New York, 1982; p 196.

(32) Collman, J. P.; Barnes, C. E.; Swepton, P. N.; Ibers, J. A. *J. Am. Chem. Soc.* **1984**, *106*, 3500.

(33) Wilson, C. R.; Taube, H. *Inorg. Chem.* **1975**, *14*, 2276.

[Rh$_2$(OAc)$_4$(CH$_3$OH)$_2$] were made following the method of Wilkinson et al.[20] All operations were carried out under argon, by using classical Schlenk tube techniques.

Na[Rh$_2$(OAc)$_3$(dcnp)]. In a 50-mL two-neck flask equiped with a condenser, NaOH (36.4 mg, 0.91 mmol) and dcnpH$_2$ (100 mg, 0.45 mmol) were dissolved in 35 mL of CH$_3$OH at room temperature. [Rh$_2$(OAc)$_4$(CH$_3$OH)$_2$] (244 mg, 0.47 mmol) was added under argon, and the mixture was refluxed with stirring for 16 h. The initially green color gradually turned red. After the solution was cooled to room temperature, the mixture was filtered. The filtrate was evaporated under vacuum to half of its initial volume, and 50 mL of diethyl ether was slowly added. The red precipitate that formed was collected on a frit and dried under vacuum. Yield = 78% (225 mg). ^{1}H NMR (200 MHz, DMSO-d_6): δ 8.65 (d, J_{34} = 8.4 Hz, 2 H), 8.32 (d, J_{56} = 8.4 Hz, 2 H), 2.02 (s, 3 H, trans OAc), 1.49 (s, 6 H, cis OAc). Anal. Calcd for Rh$_2$C$_{16}$H$_{17}$N$_2$O$_{12}$Na (Na[Rh$_2$(OAc)$_2$(dcnp)]·2H$_2$O): C, 29.20; H, 2.60; N, 4.25. Found: C, 29.74; H, 3.03; N, 4.10.

[Ru$_2$(OAc)$_3$(dcnp)]. In a two-neck flask with a magnetic stirring bar, NaOH (86 mg, 2.15 mmol) and dcnpH$_2$ (234 mg, 1.07 mmol) were dissolved in 30 mL of H$_2$O. [Ru$_2$(OAc)$_4$]Cl (508 mg; 1.07 mmol) was dissolved in hot MeOH (90 mL) in another two-neck flask. The solutions were degassed, and the ligand solution was slowly added to the [Ru$_2$(O-Ac)$_4$]Cl solution. An instantaneous color change (red-brown to deep blue) was observed. The mixture was stirred at room temperature for 24 h. After filtration, the solution was vacuum evaporated to one-third of its initial volume and 60 mL of diethyl ether was added. The mixture was allowed to stand overnight in the refrigerator, and the blue precipitate formed was collected by filtration and dried under vacuum. Yield = 51% (345 mg). Crystals were grown by slow evaporation of a CH$_3$-CN–CH$_3$OH (20/80) solution. Anal. Calcd for Ru$_2$C$_{16}$H$_{17}$O$_{12}$N$_2$ [Ru$_2$(OAc)$_3$(dcnp)]·2H$_2$O): C, 30.43; H, 2.69; N, 4.56. Found: C, 29.53; H, 2.67; N, 4.45.

Structure Determination. A parallelepiped-shaped crystal of approximate dimensions 0.17 × 0.3 × 0.2 mm was mounted on a thin glass fiber with epoxy. During the first attempt at data collection, large instabilities in the standard reflections were observed; therefore, the crystal was enclosed in a nitrogen-filled capillary tube for full data collection. The orthorhombic unit cell constants were determined from 25 centered reflections by using a Crystal Logic controlled Huber four-circle diffractometer[34] (Mo Kα radiation: λ = 0.71069 Å), which gave refined lattice parameters of a = 16.013 (2), b = 20.792 (3), and c = 23.264 (3)Å. A total of 5843 unique data were collected by using the θ–2θ scan mode for 2θ = 0–45°. During data collection the five standard reflections monitored for intensity variation showed no overall change; however, some instability was observed that could not be correlated with crystal motion, room temperature or any other factors. Full data collection and refinement parameters are listed in Table III.

Following data reduction, and the usual corrections for Lorentz and polarization effects, there were 2812 observed reflections according to

the criterion $I > 3\sigma(I)$. Systematic absences (0kl, $k + l \neq 2n$; $h0l$, $h \neq 2n$; 0k0, $k \neq 2n$; 00l, $l \neq 2n$) were consistent with space groups *Pnam* (No. 62) and *Pna2$_1$* (No. 33). The centric space group with 1$^1/_2$ molecules in the asymmetric unit was chosen for the initial structure determination. The ruthenium atom positions were located by the direct-methods program SHELXS-86,[35] and the light-atom positions were progressively located by Fourier difference syntheses following positional and thermal parameter refinement of the known atoms. All the least-squares and subsidiary calculations were performed by using the Oxford CRYS-TALS system.[36] The refinement led to some chemically unreasonable distances and angles in one of the independent molecules (Ru(2)–Ru(3)) in the unit cell; consequently, some C–C and C–N bond distance and bond angle restraints were included in the refinement to stabilize the model. On anisotropic refinement, some of the thermal parameters in the Ru(2)–Ru(3) molecule refined to grossly asymmetric values, and these were rerefined isotropically. Hydrogen atoms were located geometrically, and in the last cycles of refinement, their positions were optimized by riding on the their respective carbon atoms (d(C–H) = 1.0 Å), which led to final residuals of R = 7.99% and R_w = 9.76%, using a Tukey–Prince three-term weighting scheme.[37] A Larson-type extinction correction[38] was also included in the final cycles of refinement.

Because of the problems encountered in the refinement in the centric space group, refinement was also attempted in *Pna2$_1$*. This led to severe correlation between the symmetry-decoupled parameters, and even with bond distance restraints, the refinement tended to oscillate rather than converge. A reexamination of the centric model did not reveal any additional features that could be reasonably modeled by static disorder. The problems in the Ru(2)–Ru(3) unit may be caused by dynamic disorder, and we hope to perform experiments at low temperature to clarify this point. However, atomic connectivity has been unambiguously determined.

Supplementary Material Available: Table V (atomic positions), Table VI (bond distances), Table VII (bond angles), Table VIII (anisotropic thermal parameters), and Table IX (experimental details of the crystal structure) (12 pages); Table X (observed and calculated structure factors (18 pages). Ordering information is given on any current masthead page.

(34) Carruthers, J. R.; Watkin, D. J. *Acta. Crystallogr.* **1979**, *A35*, 698.

(35) Sheldrick, G. M. *SHELXS-86 Users Guide*; Institut für Anorganische Chemie: Gottingen, FRG, 1986.

(36) Watkin, D. J.; Carruthers, J. R.; Betteridge, P. W. *CRYSTALS User Guide*; Chemical Crystallography Laboratory: Oxford University, UK, 1985.

(37) Carruthers, J. R.; Watkin, D. J. *Acta Crystallog.* **1979**, *A35*, 698.

(38) Larson, A. C. In *Crystallographic Computing*; Ahmed, F. R., Ed.; Munksgaard: Copenhagen, 1970; p 291.